3D fabrication of Shape-Memory polymer networks based on coumarin Photo-Dimerization

Belkacem Tarek Benkhaled, Kedafi Belkhir, Thomas Brossier, Camille Chatard, Alain Graillot, Barbara Lonetti, Anne-Françoise Mingotaud, Sylvain Catrouillet, Sébastien Blanquer, Vincent Lapinte

3D Fabrication of Shape-Memory Polymer Networks Based on Coumarin Photo-Dimerization

Belkacem Tarek Benkhaled[1], Kedafi Belkhir[1,2], Thomas Brossier[1], Camille Chatard[3], Alain Graillot[3], Barbara Lonetti[4], Anne-Françoise Mingotaud[4], Sylvain Catrouillet[1], Sébastien Blanquer[1], Vincent Lapinte[1]*

[1]: ICGM, University of Montpellier, CNRS, ENSCM, Montpellier, France

[2]: Univ. Lille, CNRS, INRAE, Centrale Lille, UMR 8207 – UMET – Unité Matériaux et Transformations, F-59000 Lille, France

[3]: Specific Polymers, Parc Via Domitia, 150 Avenue des Cocardières, 34160, Castries, France

[4]: IMRCP, Université de Toulouse, CNRS UMR 5623, Université Paul Sabatier, 118 route de Narbonne, F-31062, Toulouse Cedex 9, France

Abstract

Photo-crosslinked shape-memory polymer (SMP) materials were obtained by the copolymerization of methacrylates bearing 2-ethylhexyl plasticizing group (EHMA) and photoactive coumarin unit (CoumMA). The photo-dimerization of coumarin units ensured the crosslinking of P(EHMA-*co*-CoumMA) and further allowed the fabrication by stereolithography of well-defined butterfly with ribbed wings to illustrate the potential of promising coumarin chemistry in additive fabrication. The influence of dye ratio on the optical and the mechanical properties of the transparent P(EHMA-*co*-CoumMA) films as well as the shape memory properties of the films in unfolding and twisting deformations were detailed and demonstrate the opportunity of coumarin-bearing photoprintable polymers for 4D printing.

Introduction

Shape-memory polymers (SMP)s (*e.g.* shape-memory thermal transition) are a class of materials capable to return to their original (permanent) shape from a deformed (temporary) one, in response to an external stimulus. For example, thermal transition shape-memory polymers maintain their temporary shape below a transition temperature (T_g or T_m) and recover their permanent shape by heating. To satisfy such typical behavior, the SMP must provide a combination of: i/ irreversible network, to fix the system and guarantee the permanent shape, with ii/ a reversible network which can be obtained by the weak interactions between the polymer chains and will insure the temporary state. The shape recovery is due to the entropy elasticity induced by the permanent network. The reversible deformation including contraction, elongation and bending can be used to remotely animate objects as robots, artificial muscles and actuators but well-defined objects are required. Recently, the development of additive manufacturing such as stereolithography (SLA) revolutionized this approach and allows the fabrication of sophisticated objects with high porosity or complex geometry.[1,2] This SLA consists in the photo-crosslinking of a polymer resin bearing photoactive units like methacrylate or epoxy. However, the family of photo-dimerizable units like anthracene, stilbene, cinnamoyl and coumarin[3] is increasingly investigated in the field of photo-curing polymer. Indeed, they present the considerable advantage to reversibly dimerize without any photo-initiator to activate the crosslinking is a considerable advantage.[4] Other photoinitiator-free initiator systems like electron-donor-acceptor tandem by using bismaleimides (BMI) as electron acceptors[5] , thiol-ene photoclick reaction[6] have also been employed for the crosslinking of polymeric materials. We selected photochromic coumarins due to their easy functionalization, simple reversible dimerization and easy accessibility on the chemical marketed.[7,8] SMPs based on coumarin chemistry were already reported with poly(ε-caprolactone)[9,10,11], polyimide[12], poly(vinyl alcohol)[13] or polyurethane[14,15], however none of them have been used in 3D printing with SLA. Our system is based on coumarin functionalized

by methacrylate moiety. This monomer is copolymerized with a 2-ethylhexyl methacrylate (EHMA) to obtain a polymethacrylate backbone P(EHMA-*co*-CoumMA). EHMA acts as internal plasticizer allowing material deformations essential to recover the initial shape after heating above glass temperature (Figure 1). The homologous acrylate copolymers in acrylate series were already described by Lon et al.[16] for photoreactive pressure-sensitive adhesives (PSA) application. However, they employed another synthetic route. First, they copolymerized 2-ethylhexyl acrylate and 2-hydroxyethyl acrylate before modifying a part of alcohol groups with 7-chlorocarbonylmethoxycoumarin. In addition, P(EHMA-*co*-CoumMA) has already been reported by Demirelli et al.[17] without any description of the resulting materials even if they demonstrated through a kinetic study on the copolymerization the ideal character of P(EHMA-*co*-CoumMA) with a r=0.45 for coumarin monomer. The use of polymers bearing photoactive coumarin units in SLA was only reported by Matsuda et al.[18] and never used to fabricate SMP materials. Consequently, we investigated in this study the SMP properties of P(EHMA-*co*-CoumMA) synthesized with various ratios of CoumMA and the casted on large-scale photo-crosslinked films. We further used P(EHMA-*co*-CoumMA) in SLA. A butterfly design presenting SMP properties was built as a proof of concept by SLA.

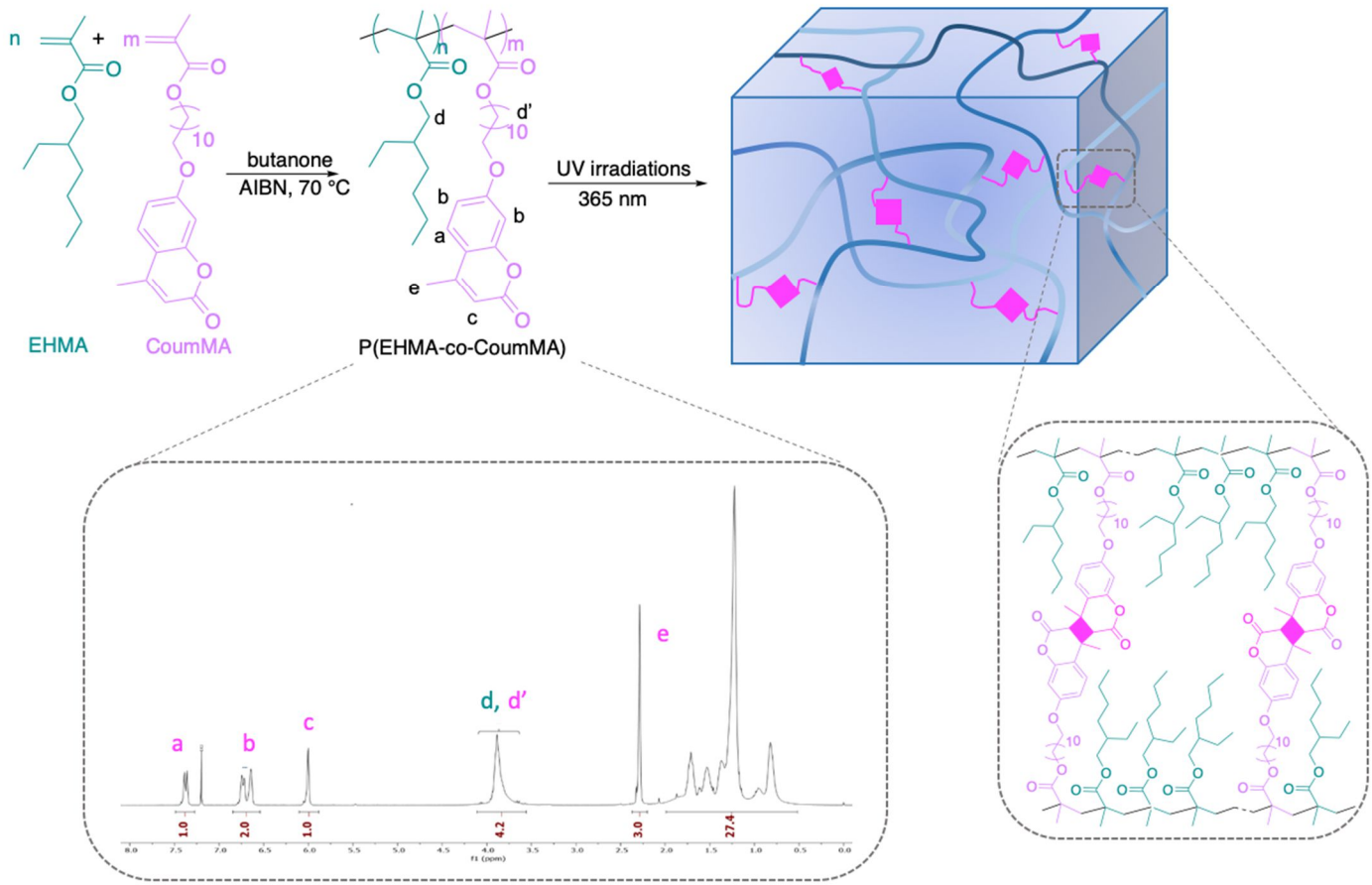

Figure 1. Synthesis of P(EHMA-*co*-CoumMA) by radical polymerization followed by its photo-crosslinking using coumarin dimerization.

Material and methods

Material

4-Methylumbelliferone, 11-bromoundecanol, 2-ethylhexyl methacrylate (EHMA), methacrylic acid (MA), triethylamine (TEA), 2,2′-azobis(2-methylpropionitrile) (AIBN), Darocur 1173, dichloromethane (DCM), ethanol (EtOH), butanone, $MgSO_4$, and potassium carbonate (K_2CO_3) were purchased from Aldrich and used without further purification.

Characterization

^1H and ^{13}C spectra were recorded in $CDCl_3$ using a Bruker Advance DRX 400 (400 MHz). For ^1H NMR, chemical shifts were referenced to the peak of residual non-deuterated solvent at 7.26 ppm for $CDCl_3$. Molar masses and dispersity of polymers were determined by size exclusion chromatography (SEC) using a PL-GPC50 Plus equipped with a RI refractive index detector. Polar Gel M column was used at 50 °C with dimethylacetamide (DMAc) (+0.1% LiCl weight) flow rate of 0.8 $mL.min^{-1}$, calibrated with PMMA standards. UV-dimerization of the coumarinated films was performed in a cylindrical photochemical reactor ‘‘Rayonnet RPR-200’’ equipped with 16 symmetrically placed lamps with emission maximum at 350 nm (UV-B). UV-visible analyses were conducted using a Perkin Elmer lambda 35 UV-visible spectrometer equipped with a PTP-1 + 1 Peltier system in quartz vial (length = 1 cm). A small lamellar film was introduced in quart z cell to follow the kinetic of crosslinking (dimerization of coumarin moieties). DSC analyses were carried out using a Mettler Toledo (Mettler Toledo, France) DSC1 calorimeter. Nitrogen was used as the purge gas. Thermal properties were recorded between 0 and 60 °C at a heating rate of 5 $°C.min^{-1}$. The stress-strain measurements on films were performed using an Instron 5533 tensile tester equipped with a 10 KN static load cell and specimen gripe. The results were interpreted on a Bleuhill3 software. The tensile measurements were performed zed on the lamellar shape films (1.5x15 cm) according to the

ISO's norms (ISO 527-3). The traction rate of samples was 1 mm/s for all the runs, with 0.1N preload. Three samples were used to obtain the average data. The tensile modulus (Young's modulus) was calculated as the slope in the linear region of the stress-strain curve corresponding to 5–10% strain (following the ISO's norm ISO-844 2014) using the equation 1:

$$E = \frac{\delta}{\varepsilon} \quad (1)$$

with E the Young's modulus (Pa), δ the stress (Pa) calculated from the equation σ = F/S, where F is the force (newton) and S the nominal cross-section (or surface) of the sample (m^2).

Synthesis of 7-(11-acryloyloxyundecyloxy)-4-methyl coumarin (CoumMA)

Step 1. Synthesis of 7-(11-hydroxyundecyloxy)-4-methyl coumarin (CoumOH)

In a single-neck round-bottom flask, 7-hydroxy-4-methylcoumarin (39.0 g, 0.22 mol) was dissolved in 675 mL of ethanol. Potassium carbonate (33.0 g, 0.24 mol, 1.1 eq) and 11-bromo-1-undecanol (50.0 g, 0.20 mol, 0.9 eq) were then successively added. The mixture was stirred at 85 °C for 72 hours. The mixture was filtered to remove insoluble salts. The filtrate was then concentrated under vacuum, and the yellow solid was dissolved in 900 mL of dichloromethane. The solution was washed with 3x150 mL of NaOH 1M, 1x150 mL of HCl 0.5M and 1x150 mL of deionized water. The organic phase was dried over anhydrous sodium sulfate, then concentrated under vacuum until no solvent remained. The beige solid was triturated in 1L of diethyl ether, then filtrated and dryed under vacuum at room temperature, CoumOH was obtained as a white powder in 82% yield (56.7 g).

^{1}H NMR ($CDCl_3$) δ (ppm): 7.51 (d, 1H), 6.85 (dd, 1H), 6.80 (d, 1H), 6.13 (d, 1H), 4.01 (t, 2H), 3.65 (t, 2H), 2.40 (d, 3H), 1.81 (quint, 2H), 1.66-1.22 (br, 18H). (Figure S1)

Step 2. Methacrylation of 7-(11-hydroxyundecyloxy)-4-methylcoumarin (CoumMA)

In a two-neck round-bottom flask, CoumOH (56.7 g, 0.164 mol) was dissolved in 300 mL of dichloromethane. Triethylamine (19.9 g, 0.196 mol, 1.2 eq) was then added. The mixture was cooled down to 0 °C with an ice bath, and methacryloyl chloride (18.8 g, 0.180 mol, 1.1 eq) was added dropwise under argon. When the addition was complete, the ice bath was removed and the mixture was stirred at room temperature for 1 h. The mixture was diluted in 900 mL of dichloromethane, and the solution was successively washed with 2x150 mL of HCl 0.5M, 2x150 mL of NaOH 1M and 1x150 mL of deionized water. The organic phase was dried over anhydrous sodium sulfate, then concentrated under vacuum. CoumMA was obtained as a white powder in 89% yield (60.6 g).

^{1}H NMR ($CDCl_3$) δ (ppm): 7.51 (d, 1H), 6.85 (dd, 1H), 6.81 (d, 1H), 6.13 (d, 1H), 6.11 (m, 1H), 5.56 (quint, 1H), 4.15 (t, 2H), 4.02 (quint, 1H), 2.40 (d, 3H), 1.95 (t, 3H), 1.82 (quint, 2H), 1.68 (quint, 2H), 1.55-1.20 (br, 14H). (Figure S2 (a))

^{13}C NMR ($CDCl_3$) δ (ppm): 167.53, 162.24, 161.32, 155.32, 152.54, 136.56, 125.44, 125.09, 113.39, 112.66, 111.80, 101.34, 68.60, 64.80, 29.48, 29.46, 29.31, 29.21, 28.98, 28.60, 25.95, 18.63, 18.31. (Figure S2 (b))

Typical procedure for the synthesis of P(EHMA-*co*-CoumMA) copolymers

Three amorphous statistical copolymers with different composition P($EHMA_{80}$-*co*-$CoumMA_{20}$), P($EHMA_{50}$-*co*-$CoumMA_{50}$) and P($EHMA_{80}$-*co*-$CoumMA_{20}$)) were successfully synthetized. The protocol is illustrated with P($EHMA_{80}$-co-$CoumMA_{20}$) synthesis.

In a two-neck round-bottom flask, CoumMA (11.0 g, 26.5 mmol) was dissolved in 60 mL of butanone. 2-Ethylhexyl methacrylate (21.1 g, 0.106 mol) and AIBN (0.22 g, 1.3 mmol) were added. The mixture was deoxygenated by argon flow for 10 min at room temperature, then heated at 70 °C overnight to perform the polymerization. When the maximal conversion rate

was reached (97%), the mixture was cooled down to room temperate. Then, the polymer was precipitated in 1.3 L of a mixture EtOH/Et_2O 95/5 v/v, and let to settle before removing the supernatant solvent. Next, the product was dissolved in dichloromethane and concentrated under vacuum. PEHMA-co-CoumMA was obtained as a white powder in 79% yield (25.2 g).

^{1}H NMR ($CDCl_3$), δ (ppm): 7.41 (d, 1H, H_{CoumMA}), 6.82 – 6.63 (m, 2H, H_{CoumMA}), 6.05 (s, 1H, H_{CoumMA}), 4.19 – 3.36 (br, 6H, $2H_{EHMA}$ + $4H_{CoumMA}$), 2.32 (s, 3H, H_{CoumMA}), 2.07 – 0.49 (br, -CH_2 and -$CH_{3\ aliphatic}$). (Figure S3, S4 and S5 (a))

^{13}C NMR ($CDCl_3$), δ (ppm): 177.91, 177.53, 176.78, 162.24, 161.30, 155.31, 152.53, 125.44, 113.38, 112.64, 111.79, 101.32, 68.60, 67.07, 64.98, 45.16, 44.78, 38.46, 30.46, 29.62-29.33, 29.04, 28.94, 28.15, 26.01, 23.86, 22.95, 22.88, 18.63, 14.11, 10.96. (Figure S3, S4 and S5 (b))

Typical procedure of film process

An amount of P(HEMA-*co*-CoumMA) (100 g) was dissolved in 100 mL of DCM. 4 hours of stirring were required to obtain the complete dissolution of the polymer. The solution was poured in a Pyrex flat inner (15×11 cm). The solvent was evaporated first under fume hood during 12 hours, then the film was subsequently put in an oven at 60 °C for 3 hours, and finally dried in a vacuum oven at 30 °C during 1 hour. The resulting film was cross-linked under UV irradiation at 365 nm, during 3 hours.

3D printing

The resin formulation was prepared to SLA process by mixing P(EHMA-*co*-CoumMA) with a non-reactive solvent (DMAc) at 75 wt%. The solution was stirred overnight at 25 °C and yielded a homogeneous reactive solution providing an optimal pattern resolution.

3D butterfly was designed from Rhinoceros 3D using the STL format. The 3D structure was built by SLA from the resin mentioned above by using a 385 nm digital light processing (DLP)

apparatus (Asiga Max X43, Australia). The 3D objects were constructed layer-by-layer by photo-crosslinking with a thickness of 200 μm. Each layer was illuminated over an intensity of 40 mW/cm² for a specific duration of 600 s. After building, the object was washed with DCM and dried at room temperature.

Shape memory folding deployment test

Rectangular samples (1.5×15 mm) were used to test the shape memory performance of the films. The test was performed using the following steps: (i) heating the samples to a target temperature > Tg in the oven and holding them for 10 min; (ii) bending the samples into "U" shape. The "U" shaped samples were then quickly removed from the oven and frozen in an intermediary shape at room temperature with a constant external force. Later, the specimens were reheated above the thermal deformation temperature to measure the bending angle θ_i every ten seconds. The final bending angle was noted θ_{max} and defined by equations 2 and 3:

$$\text{Shape recovery ratio: } R_r = \frac{\theta_{max}-\theta_i}{\theta_{max}} \times 100 \quad (2)$$

$$\text{Shape recovery rate: } V_r = \frac{\pi \times \theta_i}{180t} \quad (3)$$

Results and discussion

A series of photoactive copolymers P(EHMA-*co*-CoumMA) was synthesized using AIBN and starting from ethylhexyl methacrylate (EHMA) and a methacrylate comonomer bearing coumarin unit in pendent position (CoumMA) (Figure 1). CoumMA was produced *via* a two-step route from umbelliferon as previously reported by our group.[19] First, a C_{11} spacer chain was grafted on umbeliferone before methacrylating the terminal alcohol group. The CoumMA monomer was produced in 100 grams range in 73% global yield. %CoumMA in P(EHMA-*co*-CoumMA) ranged from 20 to 80% with similar molecular weight ($M_{n,\,sec}$ around 45,000 g/mol) (Table S1) corresponding to 22.5, 53.75 and 86.0 coumarin units per chain. The respective EHMA and CoumMA ratios were estimated by ^{1}H NMR spectroscopy using -$\underline{CH_2}$-C-$\underline{CH_3}$- (from polymer backbone) signal at 1.9-0.6 ppm related to coum-$\underline{CH_3}$ (from coumarin moiety) signal at 2.3 ppm.

Large size films (20 x 30 cm) were molded by casting of DCM solution of each copolymer P(EHMA-*co*-CoumMA). Homogeneous films with smooth surface without any trapped air bubbles in the materials were obtained. The transparency of the films is clear on the pictures of Figure 2. No color of P($EHMA_{80}$-*co*-$CoumMA_{20}$) film was observed while a yellowing appeared progressively in the case of the P($EHMA_{50}$-*co*-$CoumMA_{50}$) and P($EHMA_{20}$-*co*-$CoumMA_{80}$) films, as illustrated in the transmittance spectra obtained using UV spectroscopy.[20] The color of materials is linked to the number of coumarin rings. Higher ratio of coumarins per chain lead to more colored films while preserving transparency. P(EHMA-*co*-CoumMA) films were characterized by DSC monitoring the glass transition temperature as shown in Figure 3B. The Tg values ranged from 1 to 17 °C for 20, 50 and 80% of coumarin units (Figure 3C) in accordance with a linear relationship with the increasing coumarin amount. The low Tg values correspond to flexible films observed at room temperature.

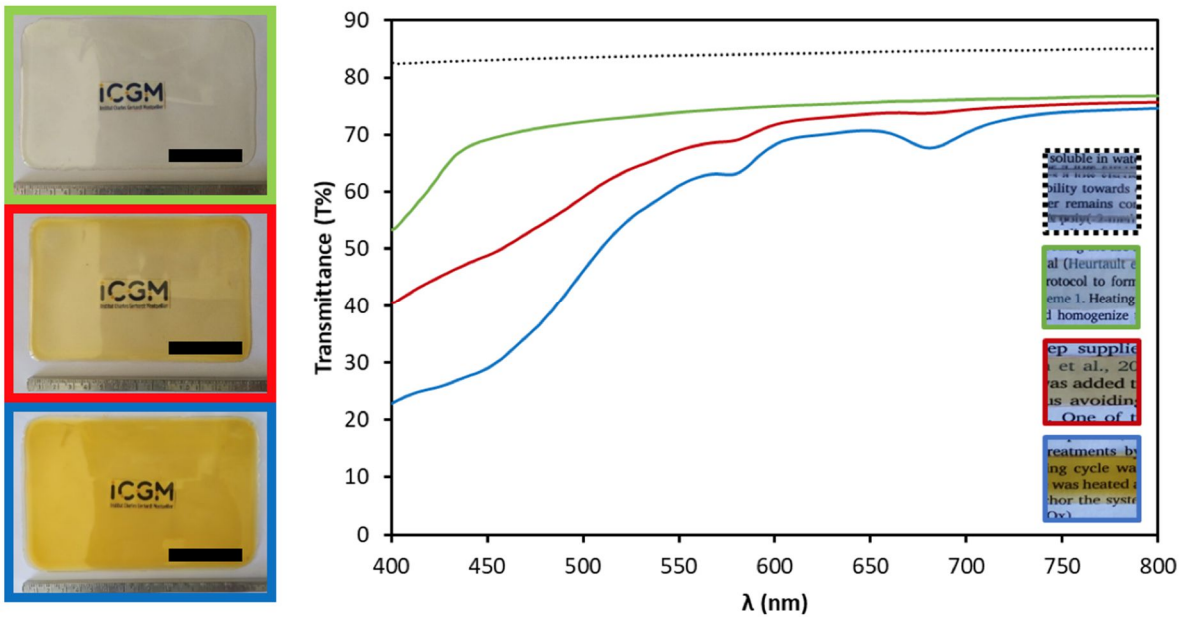

Figure 2. Images (bar: 5 cm) and transmittance spectra of the films before UV-irradiation P(EHMA$_{80}$-*co*-CoumMA$_{20}$) in green, P(EHMA$_{50}$-*co*-CoumMA$_{50}$) in red and P(EHMA$_{20}$-*co*-CoumMA$_{80}$) in blue. PMMA film as reference in black.

The photo-crosslinking of P(EHMA-*co*-CoumMA) films was undertaken under UV irradiation at 365 nm allowing the dimerization of the photoactive coumarin units according to [2+2] photo-cyclization. No warping of the films was observed during the building of the network in contrast with the material's contraction which sometimes happens during crosslinking as previously reported by Zhao et al.[21] The kinetic of the photoreaction was monitored by UV-spectroscopy as illustrated in Figure 3A with the progressive disappearance of the large band centered at 320 nm and attributed to the unsaturation of coumarin. The optimal conversion of the coumarin units into cyclobutene adducts is around 90% after 90 min of illumination instead of 60% as already reported by Long et al.[16] As expected, the photo-crosslinking induced an increase of the Tg values and consequently the stiffness as represented in Figure 3B and 3C.

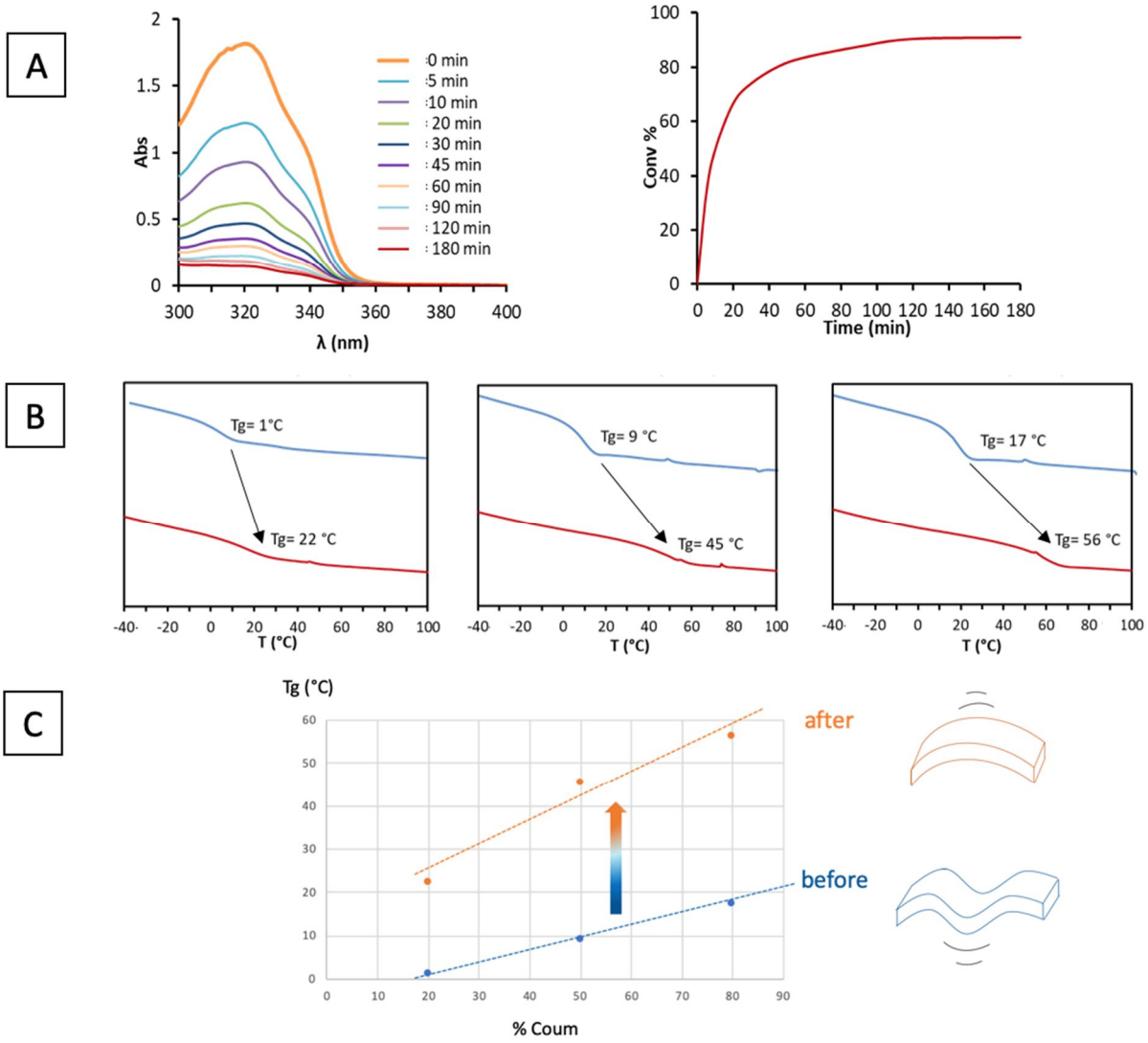

Figure 3. (a) Kinetic study of a coumarin dimerization under UV exposure at λ=365 nm monitored by UV-vis spectrometer (*e.g.* P(EHMA$_{80}$-*co*-CoumMA$_{20}$)). (b) Tg value of the films before and after photo-crosslinking using DSC. (c) Tg value of the films related to the ratio of coumarin units (the drawings illustrate the gain in stiffness by crosslinking) before in blue and after in orange UV irradiations).

Furthermore, the crosslinking of the P(EHMA-*co*-CoumMA) chains induced a quasi-linear increase of the Tg value especially high when the coumarin rate increases (Figure 3 b). A ΔTg of 21 °C for P(EHMA$_{80}$-*co*-CoumMA$_{20}$) compared to a ΔTg of 39 °C for P(EHMA$_{20}$-*co*-CoumMA$_{80}$) (Figure 3 c).

In all the cases, the Tg before crosslinking remained below room temperature which then could be a positive factor to facilitate the curing of the polymer chains under UV irradiation.[22]

The success of the photo-crosslinking paved the way for additive manufacturing by vat photo-polymerization such as the stereolithography (SLA). Using a coumarin-based resin with intermediary content of coumarin P(EHMA$_{20}$-*co*-CoumMA$_{80}$), fabrication by SLA using a DLP process was investigated. A proof of concept was chosen representing a butterfly design (37 x 25 x 3.5 mm Figure 4B clearly shows the precise reproduction of the butterfly from the STL format (Figure 4A) with all the details especially regarding the rib's design on each wing. In addition, except a slight contraction of the structure which is due to the solvent extraction, the butterfly design was preserved upon drying step (Figure 4C).

To the best of our knowledge, such performance of processing is reached for the first time by stereolithography using a coumarin-based resin. Photo-crosslinking by coumarin dimerization without using any radical initiators or small molecules is a remarkable opportunity for specific applications where the use of photo-initiator represents a serious limitation such as in biomedical applications.[23,24]

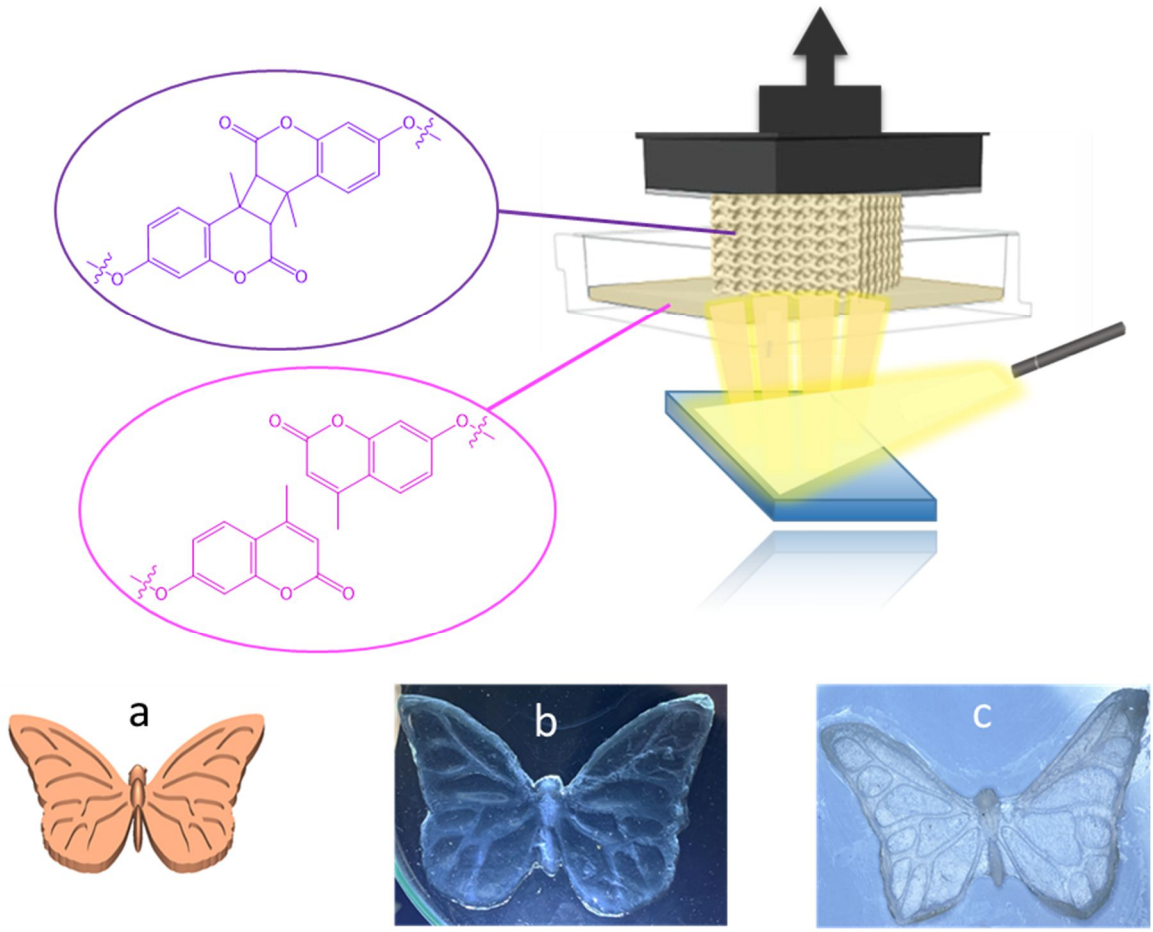

Figure 4. (a) 3D printing by stereolithography of a butterfly based on coumarin resin (*e.g.* P(EHMA$_{20}$-*co*-CoumMA$_{80}$)), photographs of the printed object (b) after printing process and (c) after drying.

Axial tensile tests were conducted to investigate the influence of the crosslinking rate on the mechanical properties of P(EHMA-*co*-CoumMA) films (Figure 5). The Young's modulus (E) of the films was deduced from the linear elastic region at low strains while the tensile strength (σ_{max}) and the fracture strain (ε_{max}) were measured at the break of the samples in the strain experiments. The films became stiffer with increasing coumarin composition as shown by the decrease of elongation at break (from 47.5 to 3.5%) as well as the increase of stress at break (from 2 to 36 MPa) and the elastic modulus ranging from 6.6 to 15.9 MPa. We noted the contrast

between the mechanical behavior of P(EHMA$_{80}$-*co*-CoumMA$_{20}$), soft and elastic material and the other materials characterized by stiff and fragile break.

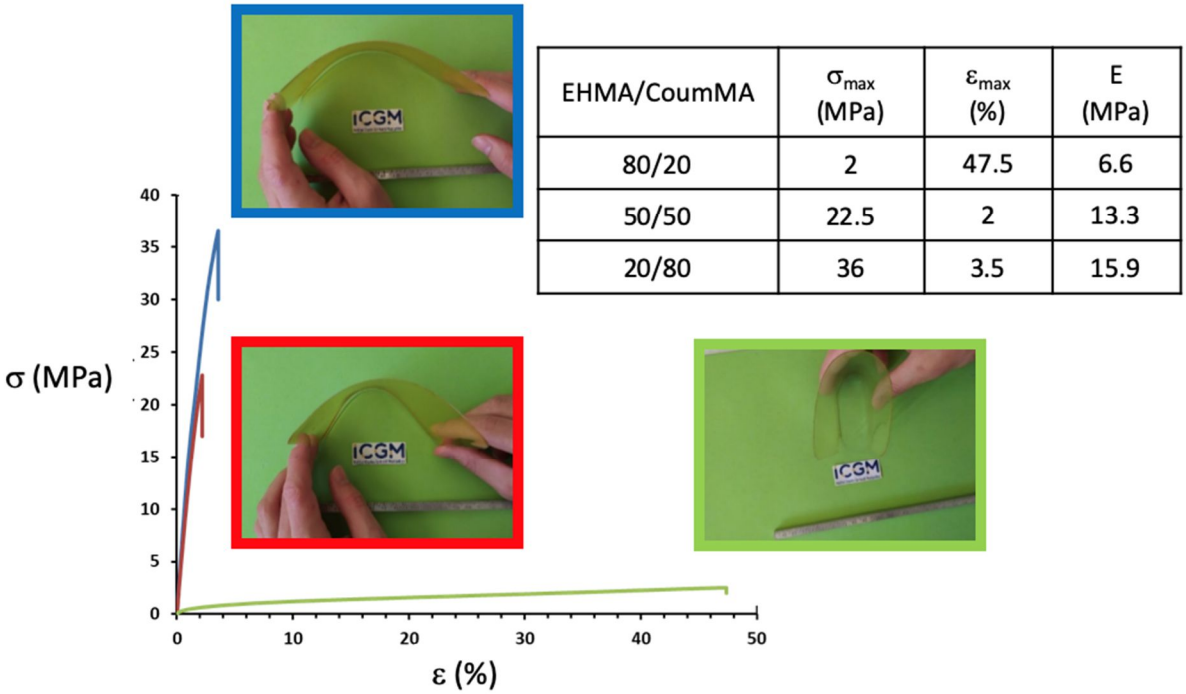

EHMA/CoumMA	σ_{max} (MPa)	ε_{max} (%)	E (MPa)
80/20	2	47.5	6.6
50/50	22.5	2	13.3
20/80	36	3.5	15.9

Figure 5. Tensile curves and images of the cross-linked films P(EHMA$_{80}$-*co*-CoumMA$_{20}$) in green, P(EHMA$_{50}$-*co*-CoumMA$_{50}$) in red, and P(EHMA$_{20}$-*co*-CoumMA$_{80}$) in blue.

SMPs are class of smart and programmable materials which have the capacity to be temporary deformed and then quickly return to their original shape upon triggered thermal stimulation at a specific transition temperature. In our case, P(EHMA-*co*-CoumMA) is amorphous, therefore the shape-morphing behavior is expected by programming around the glass transition temperature.

The resulting cross-linked materials of a crosslinking present a glass transition temperature higher than the room temperature. Hence a double network is present with a permanent covalent network due to the crosslinked nature of the material and a second network due to the weak interactions responsible for the Tg, which are reversible with temperature. Such a material can

present shape memory properties.[25] Polymers with shape memory properties feature the ability to return from a deformed state (temporary shape) to their original (permanent) shape through an external stimulation.[26] Two experiments were conducted to evidence these properties. After crosslinking, a permanent shape of flat films was obtained. The first experiment consisted in twisting the films at 80 °C, and freeze them in a temporary shape at room temperature. The experiment is illustrated with P(EHMA$_{50}$-*co*-CoumMA$_{50}$) in Figure 6A but the same behavior was observed for P(EHMA$_{80}$-*co*-CoumMA$_{20}$)) (Figure S6) and P(EHMA$_{20}$-*co*-CoumMA$_{80}$) (Figure S7). The twisted films were then heated at 80 °C and recovered their initial shape in a few seconds. To compare the speed of recovery a second experiment was conducted. The films were bent in a unidirectional deformation (Figure 6B). The deformation angles were measured at various times to determine the shape recovery ratio and shape recovery rate according to Equations 2 and 3. The experiment ended when the films recovered their initial shape. The experiments were run for the different compositions at 70, 80 and 100 °C (Figure 6C). As expected, the higher the temperature the faster the recovery was. It is clear that the composition of the polymer also has an influence on the rate of recovery. An increase in the amount of coumarin in the polymer composition led to a decrease of the rate of recovery. This result might seem counterintuitive because a higher crosslinking density would lead to a more rigid material that would recover its shape faster. However, in this case the ratio of coumarin in the polymer also affects the glass transition temperature. Thus, a lower Tg lead to a faster recovery rate probably due to easier movements of the chains to recover. A comparable behavior was already observed on epoxy polymers.[27]

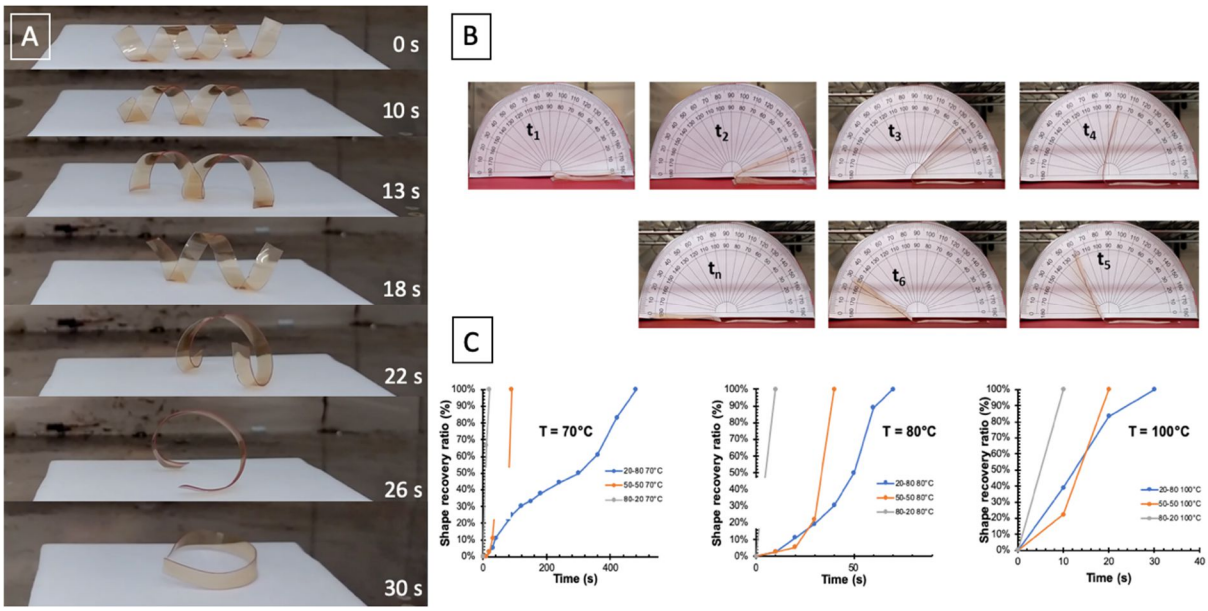

Figure 6. (a) twist of the film (*e.g.* P(EHMA$_{50}$-*co*-CoumMA$_{50}$)) at 80 °C, (b) Pictures of the unidirectional deformation of film, (c) shape recovery ratio versus time at 70, 80 and 100 °C.

As presented earlier, the polymer was successfully crosslinked using stereolithography as a proof of concept of the use of coumarin moieties for 3D printing (Figure 4). Such process opens vast applications for these polymers. But one of the issues of this process relies in the layer-by-layer printing which might compromise the shape memory properties of the material and the possible low crosslinking ratio. However, the printed butterfly kept the shape memory properties as proved by the movement of the butterfly wings in Figure 7. The initial butterfly shape was fabricated with open wings, and a temporary shape obtained by stressing the butterfly with closed wings and fixed with the temperature below the Tg, 22 °C. By applying a temperature above the Tg with an external heating we assisted to a progressive opening of the wings by simple thermal stimulation. The shape memory effect on the printed butterfly structure allows to open the perspective for such resin to be used in 4D printing.

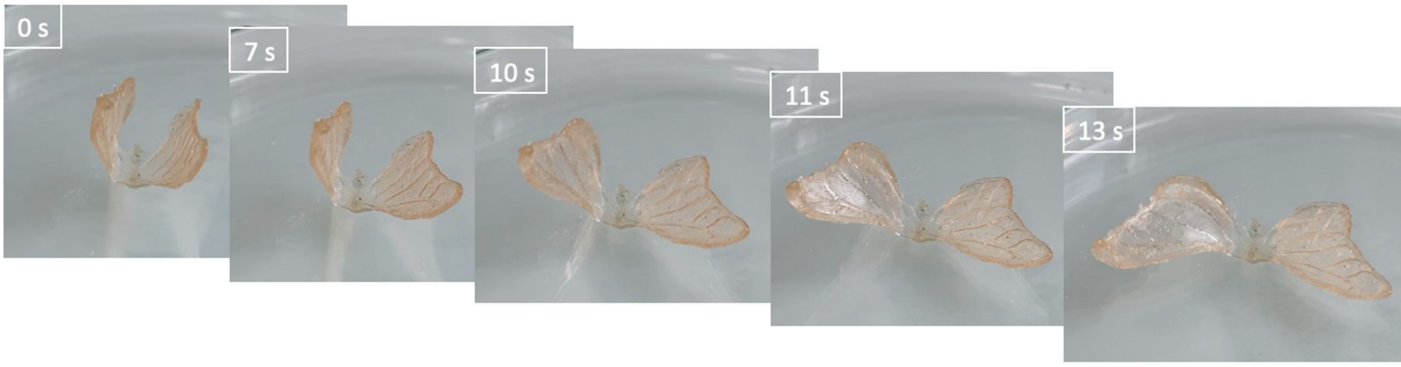

Figure 7. Movement of butterfly wings in heating (e.g. P(EHMA$_{20}$-*co*-CoumMA$_{80}$)).

Conclusion

Photo-crosslinkable polymers based on coumarin chromophore were successfully synthesized and transparent resulting films were prepared in large scale. As expected, the coumarin ratio increased the glass transition temperature of P(EHMA-*co*-CoumMA) film and its rigidity with high Young modulus and tensile strain. These thermal and mechanical properties were also amplified by photo-crosslinking. All the films exhibit thermal-induced shape memory properties as shown in unfolding and twisting deformations. Decreasing the coumarin ratio results in quicker shape memory effects. Otherwise, the study of the photodimerization of coumarins in P(EHMA-*co*-CoumMA) allows the use of these polymers as photoprintable resins in stereolithography. They demonstrate the interest of coumarin chemistry in 4D printing resulting from additive fabrication of shape memory materials as illustrated with the movement of butterfly wings during heating.

Aknowledgements

This study was achieved in the framework of the Pheophotodyn project, funded by FEDER n°LR0021768 Occitanie Region. The authors are grateful to the LMP platform of the University of Montpellier for its technical support, and thank Maxime Camas for his help.

References

[1] Blanquer S, Werner M, Hannula M, Sharifi S, Lajoinie G P R, Eglin D, Hyttinen J, Poot A. A and Grijpma D W 2017 Surface curvature in triply-periodic minimal surface architectures as a distinct design parameter in preparing advanced tissue engineering scaffolds *Biofabrication* **12** 9 2 025001.

[2] Guo Z and Zhou C 2021 Recent advances in ink-based additive manufacturing for porous structures *Additive Manufacturing Part B* **48** 102405.

[3] Sims M B, Zhang B, Gdowski Z M., Lodge T P and Bates F S 2022 Nondestructive Photo-Cross-Linking of Microphase-Separated Diblock Polymers through Coumarin Dimerization M*acromolecules* **55** 8 3317–3324.

[4] Jagtap A and More A 2021 A review on self-initiated and photoinitiator-free system for photopolymerization *Polym. Bull.*

[5] Wagner A, Mühlberger M and Paulik C 2019 Photoinitiator-free photopolymerization of acrylate-bismaleimide mixtures and their application for inkjet printing *J. Appl. Polym. Sci.* 47789.

[6] Wang Q, Chen G, Cui Y, Tian J, He M, Yang J 2017 *ACS Sustain. Chem. Eng.* **5** 376.

[7] Korchia L, Bouilhac C, Aubert A, Robin J J and Lapinte V 2017 Light-switchable nanoparticles based on amphiphilic diblock, triblock and heterograft polyoxazoline *RSC Advances* **7** 42690-42698.

[8] Korchia L, Bouilhac C, Lapinte V, Travelet C, Borsali R and Robin J J 2015 Photodimerization as an alternative to photocrosslinking of nanoparticles: proof of concept with amphiphilic linear polyoxazoline bearing coumarin unit *Polymer Chemistry* **6** 6029-6039.

[9] Defize T, Thomassin J M, Ottevaere H, Malherbe C, Eppe G, Jellali R, Alexandre M, Jérôme C and Riva R 2019 Shape Memory Behavior of Emulsion-Templated Poly(ε-Caprolactone) Synthesized by Organocatalyzed Ring-Opening Polymerization *Macromolecules* **52** 2 444–456.

[10] Nagata M and Yamamoto Y 2009 Synthesis and characterization of photocrosslinked poly(ε-caprolactone)s showing shape-memory properties *J. Polym. Sci. Part A* **47** 2422-2433.

[11] Wu Y, Hu Z, Huang H and Chen Y 2019 The design of triple shape memory polymers with stable yet tunable temporary shapes by introducing photo-responsive units into a crystalline domain *Polym. Chem.* **10** 1537-2543.

[12] Li X, Yang Y, Zhang Y, Wang T, Yang Z, Wang Q and Zhang X 2020 Dual-method molding of 4D shape memory polyimide ink *Materials & Design* **191** 108606.

[13] Zhao X, Dang Y, Deng J and Zhang 2014 Photoinduced shape fixity and thermal-induced shape recovery properties based on polyvinyl alcohol bearing coumarin *J. Colloid. Polym. Sci*. **292** 85-95.

[14] Wu Y, Huang H and Chen Y 2019 Synthesis of triple shape memory polyurethanes by introducing photo-responsive coumarin units into the crystalline soft segment *Materials Today: proceedings* **16** 1507-1511.

[15] Salgado C, Arrieta M P, Sessini V, Peponi L, Lopez D, Fernandez-Garcia M 2020 Functional properties of photo-crosslinkable biodegradabe polyurethane nanocomposites *Polymer Degradation and Stability* **178** 109204.

[16] Trenor S R, Long T E and Love B J 2005 evelopment of a light-deactivatable PSA via photodimerization The Journal of Adhesion **81** 213–229.

[17] Ayaz N, Bezgin F and Demırellı K 2012 Polymers Based on Methacrylate Bearing Coumarin Side Group: Synthesis via Free Radical Polymerization, Monomer Reactivity Ratios, Dielectric Behavior, and Thermal Stabilities International Scholarly Research Network ISRN Polymer Science **13** 352759.

[18] Matsuda T, Mizutani M and Arnold S C 2000 Molecular design of photocurable liquid biodegradable copolymers. 1. Synthesis and photocuring characteristics *Macromolecules* **33** 795-800.

[19] Oudin A, Chauvin J, Gibot L, Rols M P, Balord S, Payrée B, Lonetti B, Vicendo P, Mingotaud A F and Lapinte V 2019 Amphiphilic polymers based on polyoxazoline as relevant nanovectors for photodynamic therapy *J. Mat. Chem B.* **7** 4973-4982.

[20] Lin Y, Bilotti E, Bastiaansen C W M and Peijs T 2020 Transparent semi-crystalline polymeric materials and their nanocomposites: a review *Polym. Eng. Sci.* **60** 2351–2376.

[21] He J, Zhao Y and Zhao Y 2009 Photoinduced bending of a coumarin-containing supramolecular polymer *Soft Matter* **5** 308–310.

[22] Huyck R H, Trenor S R, Love B J and Long T E 2007 Photoinduced bending of a coumarin-containing supramolecular polymer *Journal of Macromolecular Science Part A* 45 1 9-15.

[23] You S, Miller K and Chen S 2019 Biofabrication and 3D Tissue Modeling, Ed. Dong Woo Cho **1** 1-21.

[24] Mondschein R J, Kanitkar A, Williams C B, Verbridge S S and Long T E 2017 Polymer structure-property requirements for stereolithographic 3D printing of soft tissue engineering scaffolds *Biomaterials* **140** 170–188.

[25] Behl M, Zotzmann J and Lendlein 2010 A Shape memory polymers, Advances in polymer Science book series *Polymer* **226** 1-40.

[26] Lendlein A and Kelch S 2002 Facile tailoring of thermal transition temperatures of epoxy shape memory polymers *Angew. Chem. In.t Ed.* **41** 12 2034-2057.

[27] Yu Z, Wang Z, Li H, Teng J and Xu L 2019 Shape Memory Epoxy Polymer (SMEP) Composite Mechanical Properties Enhanced by Introducing Graphene Oxide (GO) into the Matrix *Materials* **12** 7 1107.

3D Fabrication of Shape-Memory Polymer Networks Based on Coumarin Photo-Dimerization

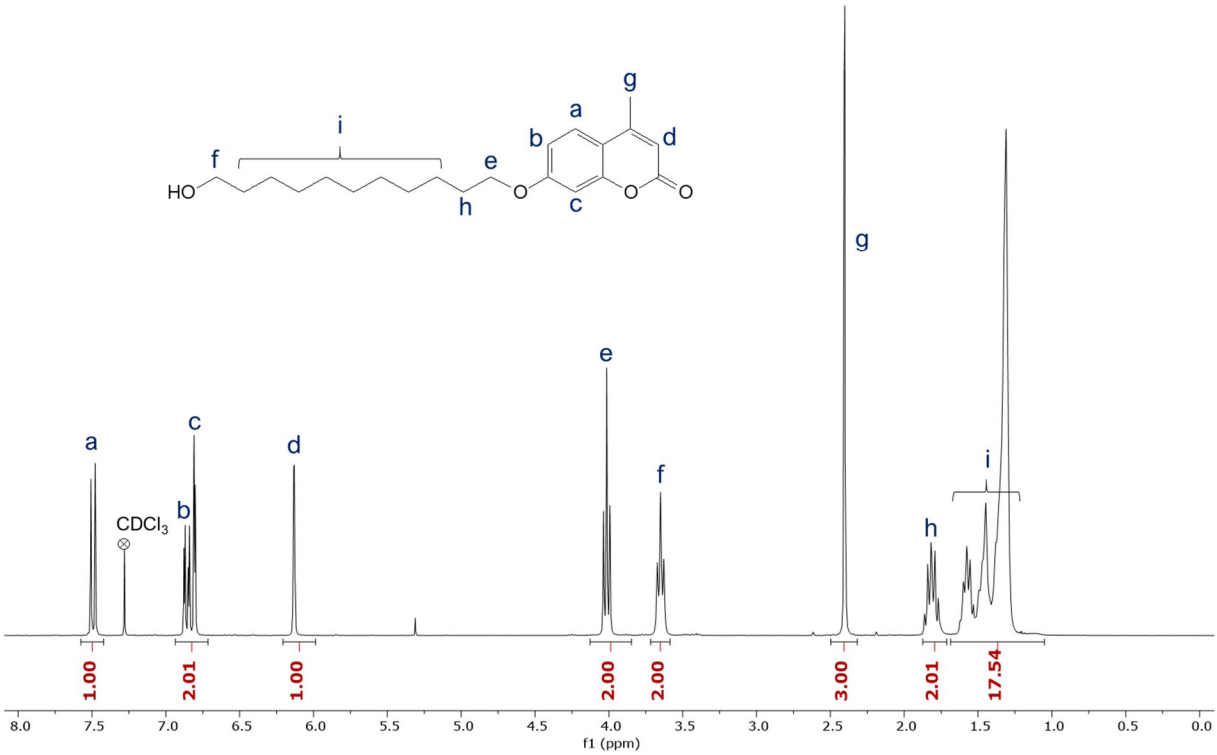

Figure S1. ^{1}H NMR spectrum of CoumOH in $CDCl_3$.

a)

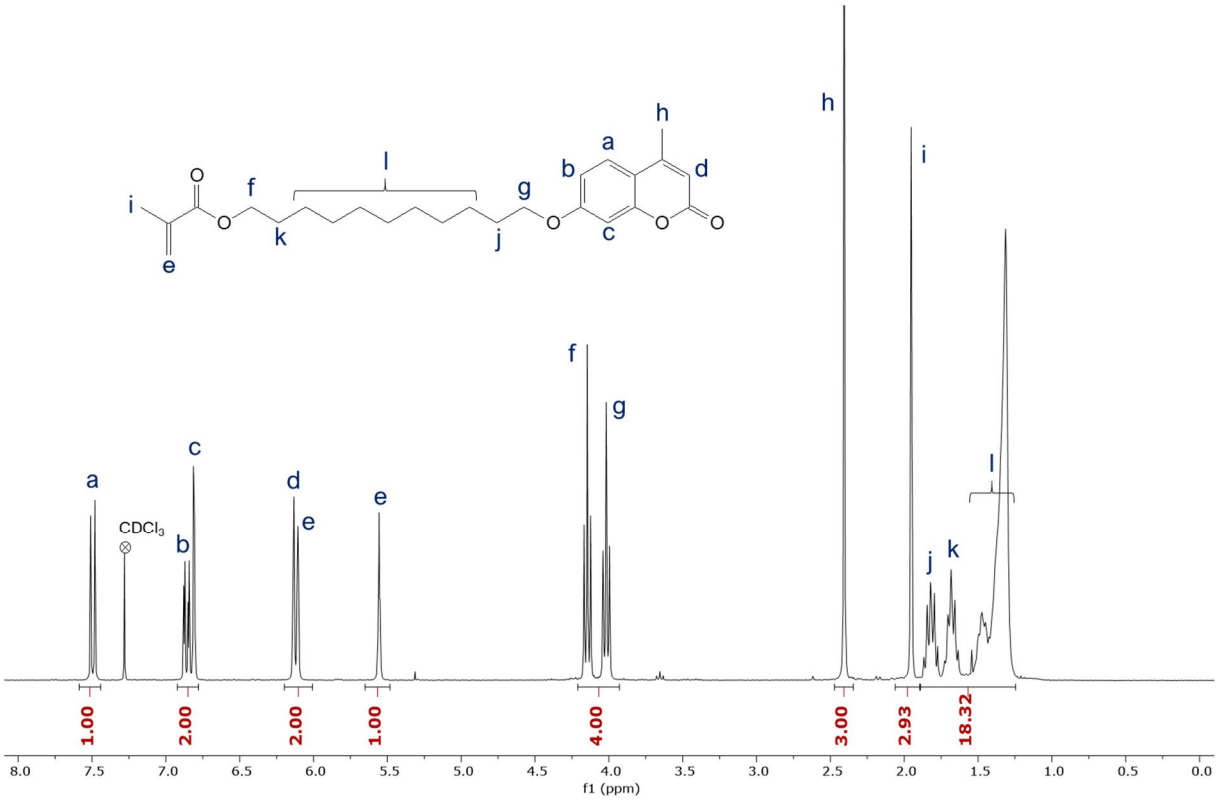

b)

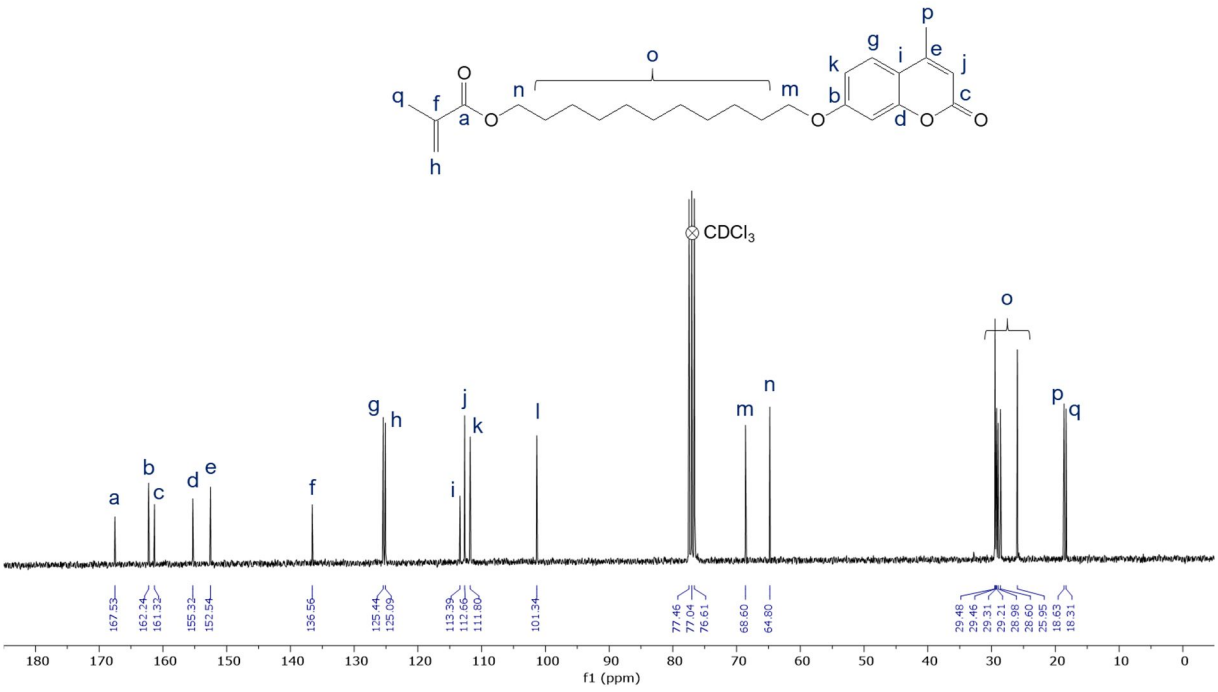

Figure S2. a) ^{1}H and b) ^{13}C NMR spectra of CoumMA in $CDCl_3$.

a)

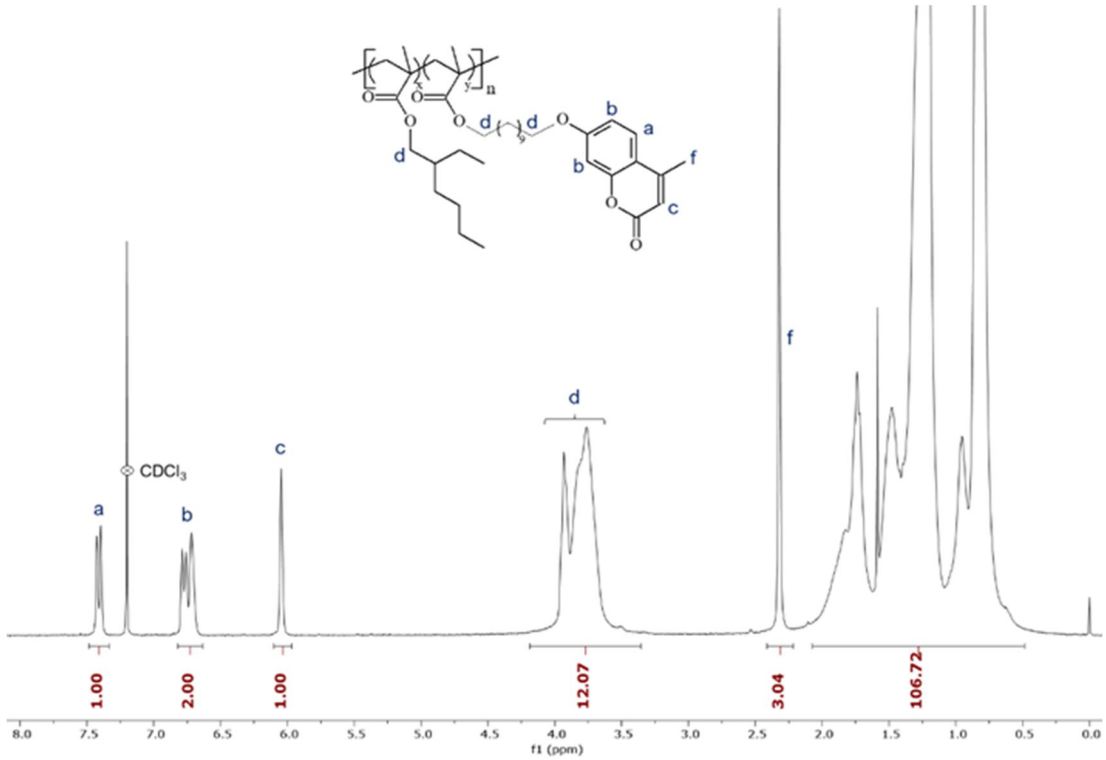

b)

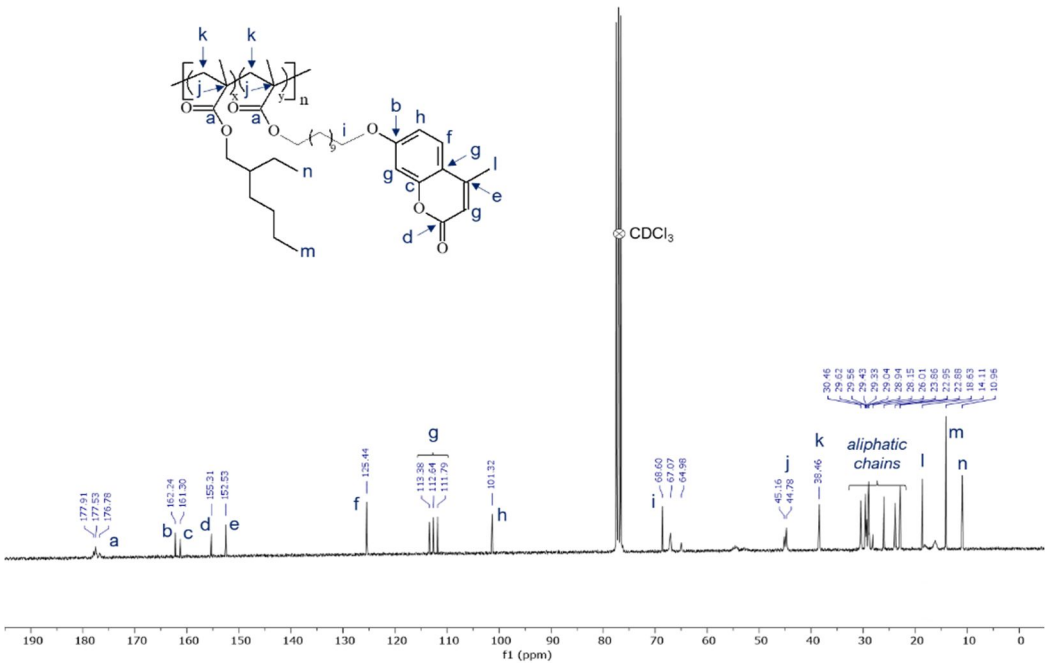

Figure S3. (a) ^{1}H and (b) ^{13}C NMR spectra of P(EHMA$_{20}$-*co*-CoumMA$_{80}$) in $CDCl_3$.

a)

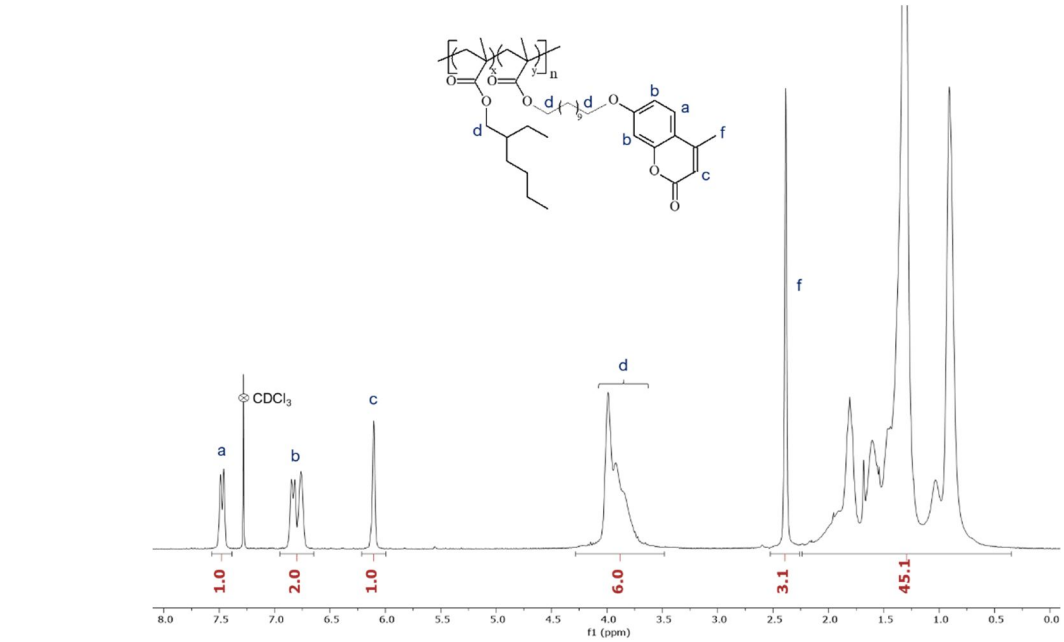

b)

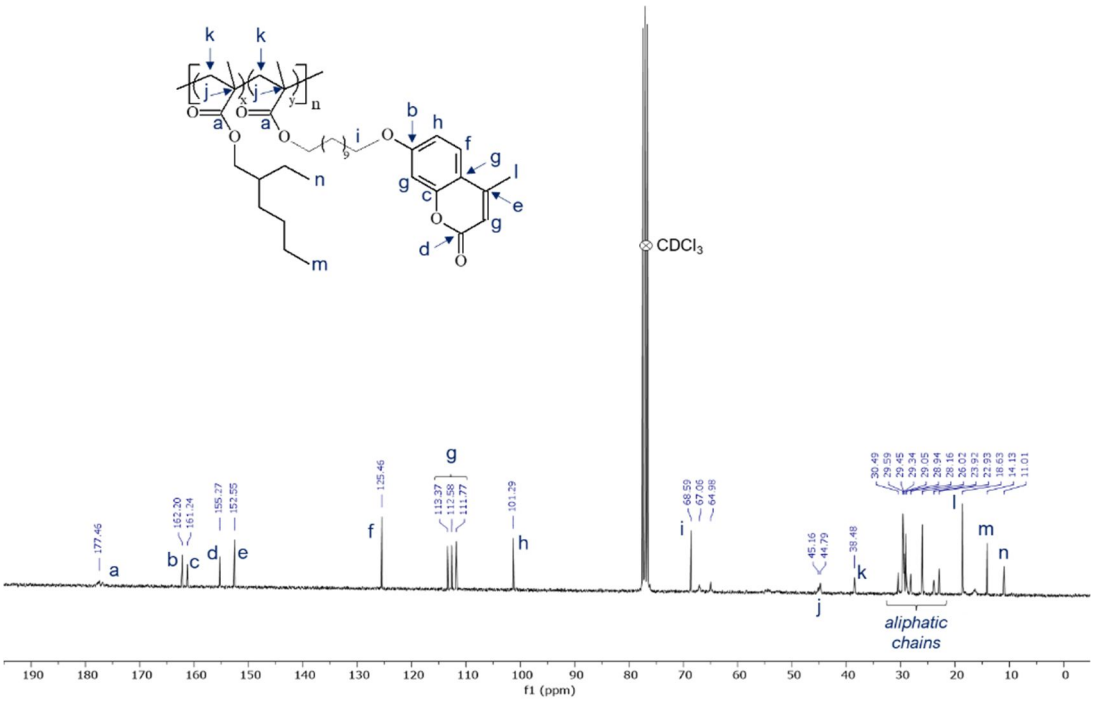

Figure S4. (a) ^{1}H and (b) ^{13}C NMR spectra of P(EHMA$_{50}$-*co*-CoumMA$_{50}$) in $CDCl_3$.

a)

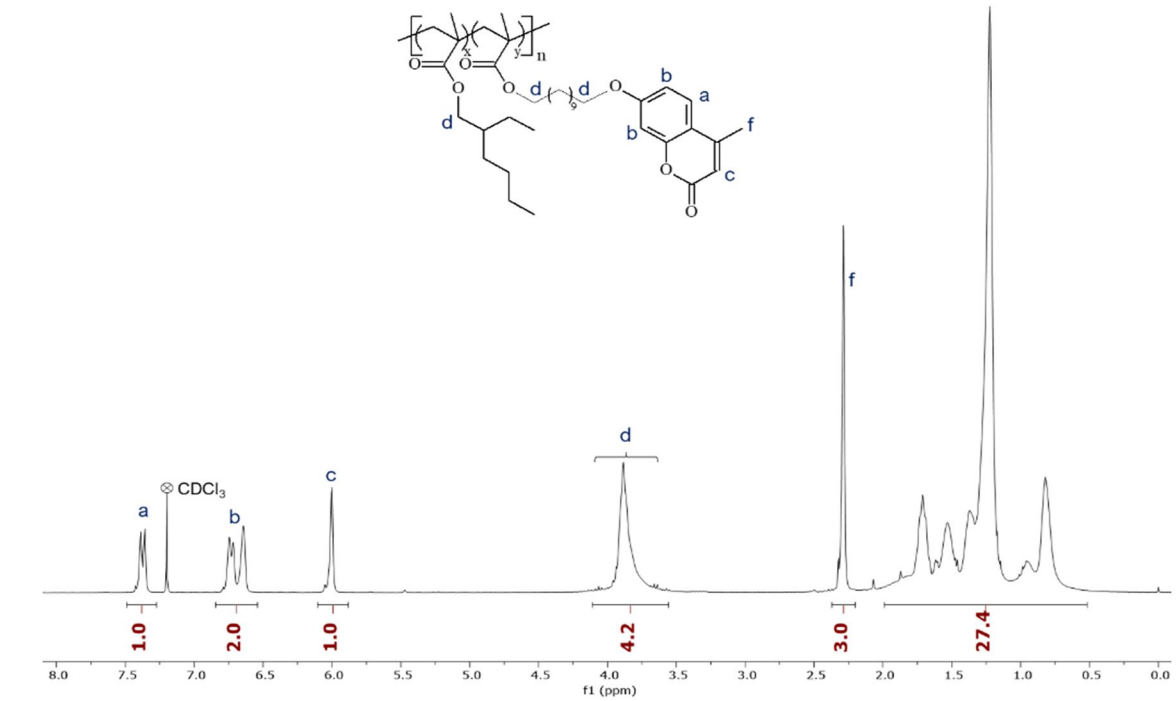

b)

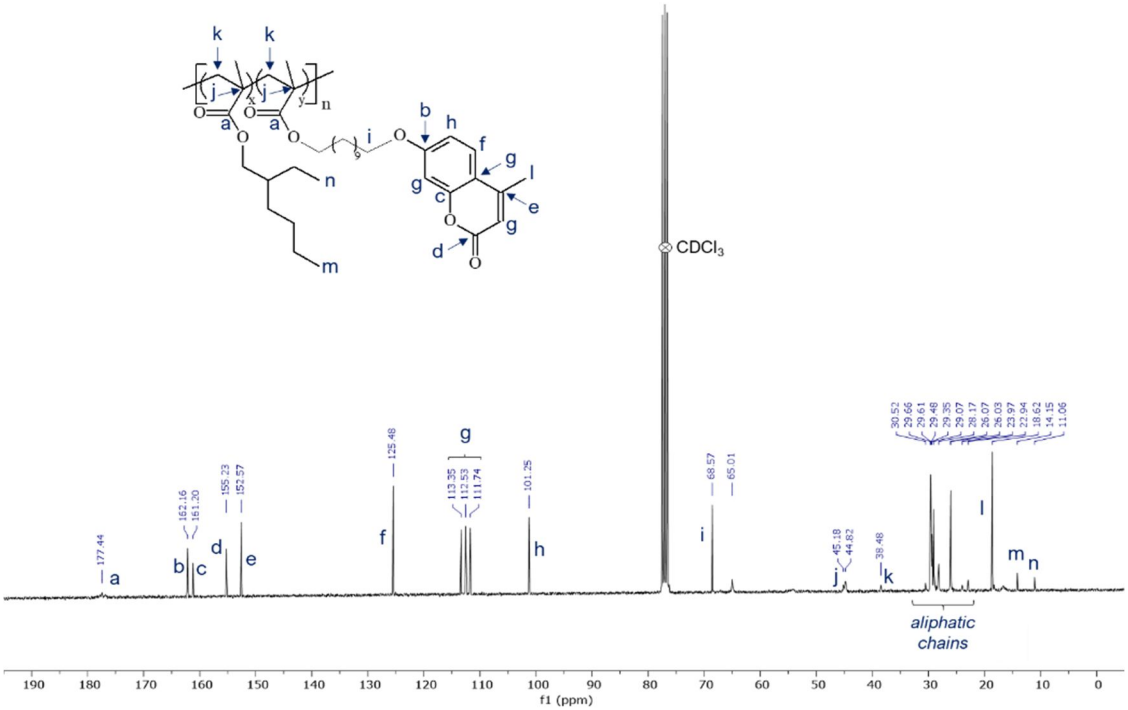

Figure S5: (a) ^{1}H and (b) ^{13}C NMR spectra of P(EHMA$_{80}$-*co*-CoumMA$_{20}$) in $CDCl_3$.

Table S1. Characteristics of P(EHMA-*co*-CoumMA).

Name	$M_{n,SEC}$ [a] ($g.mol^{-1}$)	$M_{w,SEC}$ [a] ($g.mol^{-1}$)	Ip [a]	N_{Coum} [b]	N_{HEMA} c
P($EHMA_{80}$-*co*-$CoumMA_{80}$)	45 000	127 000	2.8	22	182
P($EHMA_{50}$-*co*-$CoumMA_{50}$)	43 000	280 000	6.5	54	108
P($EHMA_{20}$-*co*-$CoumMA_{80}$)	43 000	260 000	6.0	86	43

[a]: determined by SEC using PMMA standards in DMF. [b]: $N_{coum} = (M_{n,SEC} \times \%Coum)/(M_{n\ coum}*100)$ using $\%Coum = Int(CH_3\ Coum/3H)/ Int(CH_2\text{-}C\text{-}CH_{3\ backbone}/5H)$. [c]: $N_{HEMA} = (M_{n,SEC} \times \%HEMA)/(M_{n\ HEMA}*100)$ using %HEMA = 100- %Coum.

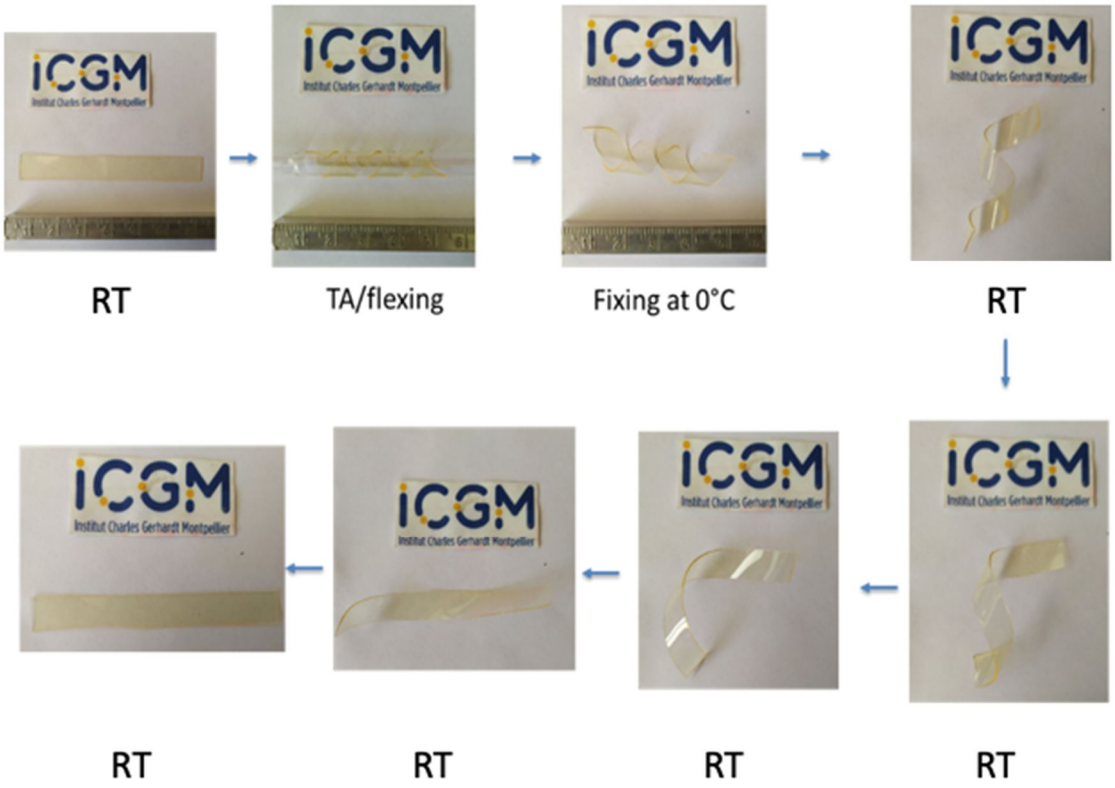

Figure S6. Shape memory of the film P(EHMA$_{80}$-*co*-CoumMA$_{20}$).

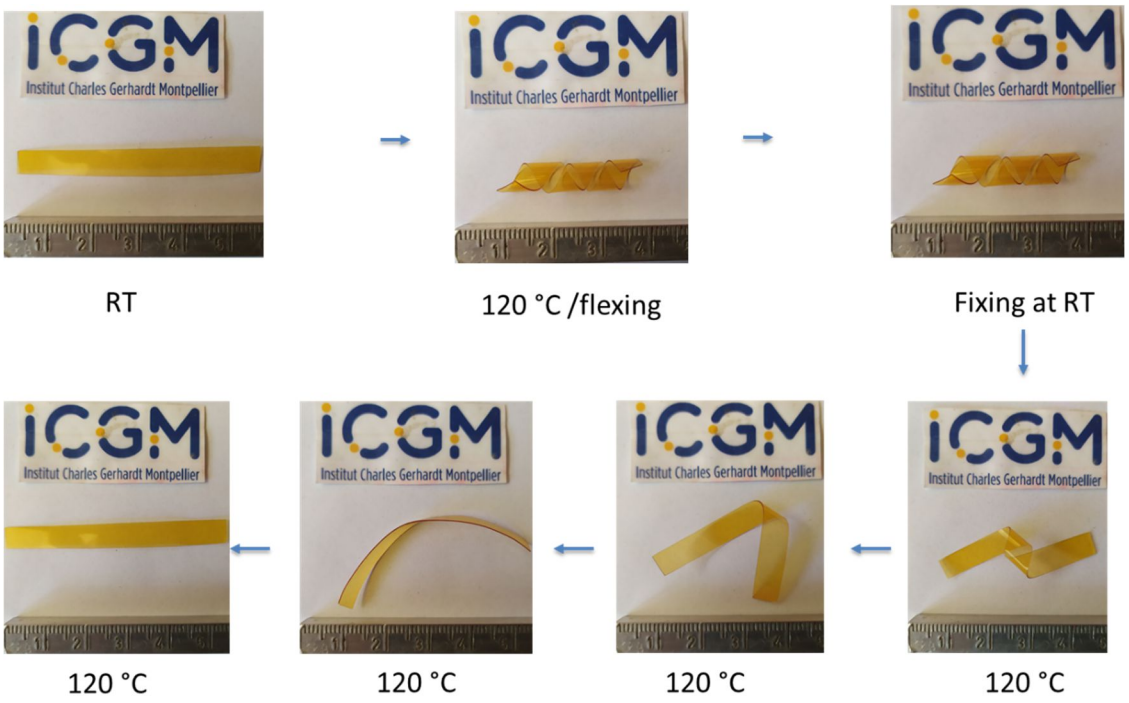

Figure S7. Shape memory of the film P(EHMA$_{20}$-*co*-CoumMA$_{80}$).